Density Functional Theory Study of the Brookite Surfaces and Phase Transitions between Natural Titania Polymorphs

A. Beltrán, L. Gracia, and J. Andrés*

Departament de Ciències Experimentals, Universitat Jaume I, Campus de Riu Sec, Castelló E−12080, Spain

Received: July 8, 2006; In Final Form: September 15, 2006

The present study is concerned with the structural and electronic properties of the low-index surfaces of the brookite form of titanium dioxide. A theoretical investigation is carried out using the density functional formalism under the nonlocal B3LYP approximation to calculate surface energies, band energy values, and to interpret the response to hydrostatic pressure of the bulk and surfaces of the brookite structure. In addition, phase transformations with pressure are predicted from the anatase and the rutile to the brookite polymorph at about 3.8 and 6.2 GPa, respectively. The orthorhombic structure and the fractional coordinates of brookite vary isotropically with the rise in pressure. The calculated band gap energy is 3.78 eV for the bulk brookite. The brookite surface stabilities follow the sequence (010) < (110) < (100), and the minimum gap energy value is found for the (110) surface.

1. Introduction

Titanium dioxide (TiO_2) has been the subject of considerable interest due to its usefulness in a wide variety of technological applications in the pigment, catalysis, electronics, electrochemical, ceramics, and solar cell industries.[1−11] TiO_2 is the most widely studied semiconductor photocatalyst for various applications, due to its high photocatalytic efficiency, chemical inertness, surface amphotericity, and nontoxicity, and also because of the multiplicity of polymorphs that it forms under varying chemical, temperature, and pressure conditions. The number of papers published has been strongly increasing through the years.

Polymorphs of TiO_2 have had considerable impact over a broad range of scientific inquiry, the most common such polymorphs being the minerals rutile, anatase, and brookite. The particular behavior of the TiO_2 polymorphs clearly depends on their crystalline form, and it has made those phases extremely useful for many applications. This variability has been attributed to differences in the rates of recombination, adsorptive affinity, or band gap energy differences between the titania phases.[12−14]

However, brookite is the rarest of the natural TiO_2 polymorphs, and it is the most difficult phase to prepare in the laboratory.[15] As a result, the properties of pure brookite are poorly known. Few studies have been reported on the synthesis of pure brookite-type TiO_2 without a mixture of rutile or anatase, at low temperature, from the X-ray powder diffraction analysis.[16,17] This fact shows the need for further characterization of this phase. Ohtani et al.[18] reported the markedly high photocatalytic activity of brookite nanocrystallites as compared to that of rutile and anatase. Koelsch et al.[19] deposited brookite as a thin film from a stable dispersion, and proposed brookite as a good candidate for photovoltaic devices. Brookite phase behavior under high temperatures was reported by Bokhimi et al,[20] where brookite and anatase phases were stable even at 700 °C while the brookite-to-rutile transformation occurred at 800 °C. However, very little information on brookite phase behavior under high pressure has been reported. A theoretical study carried out by Swamy et al.[21] predicted a bulk modulus of brookite-type TiO_2 of 211 GPa. Recently, Luo et al.[22] have studied polycrystalline brookite using energy-dispersive X-ray diffraction at pressures up to 27.8 GPa and derived a bulk modulus at ambient pressure of 255 GPa, using Birch−Murnaghan's equation of state with a fixed value of 4 as its first derivative. They found a brookite-to-baddeleyite transition between 15.8 and 22.8 GPa.

It is well-known that pressure is certainly a critical parameter for the structural stabilities, electronic and optical properties, and for the mechanism of the photocatalysis process.[23] First-principles calculations have become a powerful supplement to experimental techniques, providing reliable and accurate predictions of the structural and electronic properties of both bulk and surfaces. TiO_2 structural and electronic properties, including experimental and theoretical aspects, have been extensively studied.[24] Although the results of experiments, such as structural and elastic parameters, can be well reproduced by different theoretical approaches,[25,26] the geometric and electronic structure of TiO_2 bulk and surfaces remain an issue of debate.[27−32]

This study seeks to provide the first accurate description of the geometric and electronic structure of both the bulk and the most common surfaces of the TiO_2 brookite phase. This work discusses the results of hybrid DFT calculations on the theoretical description of the structural and electronic properties for the brookite form. The main low-index surfaces of this natural polymorph have been characterized by first-principle calculations of the surface energies and the corresponding electronic structures. The possible transformations of anatase and rutile phases into the brookite structure are also explored by analyzing the respective equations of state (EOS). The layout of this paper is as follows: Section 2 describes the bulk and surface structures of the brookite form. Section 3 sets out the computational strategy. Section 4, with two subsections, presents the theoretical results and a discussion of local compressibility and phase stability together with an electronic structure analysis for the bulk and surface structures. Finally, Section 5 summarizes the main conclusions.

* Corresponding author phone: 34-964-72-80-73; fax: 34-964-72-80-66; e-mail: andres@exp.uji.es.

10.1021/jp0643000 CCC: $33.50 © 2006 American Chemical Society
Published on Web 10/19/2006

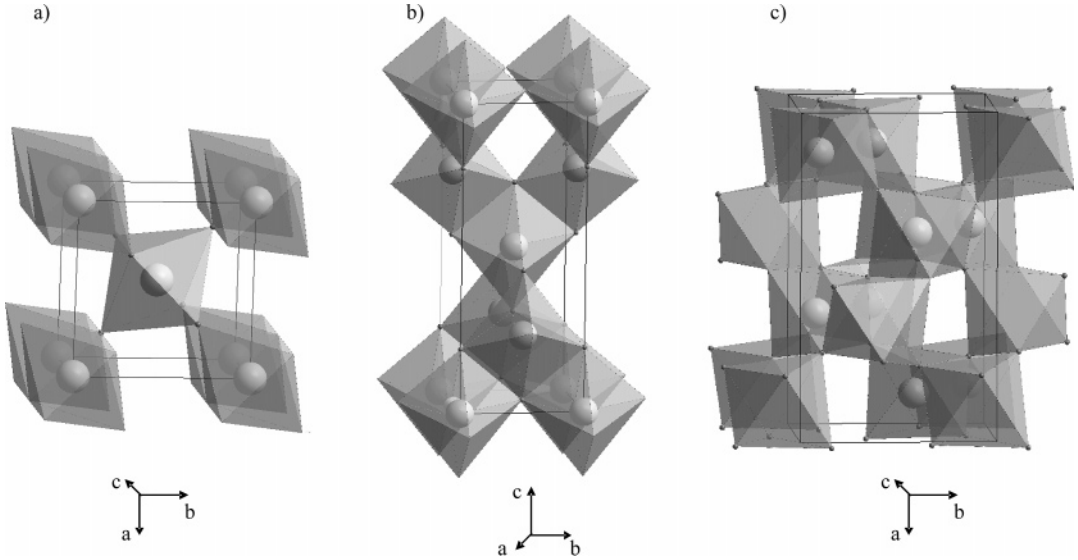

Figure 1. Bulk structures of the TiO_2 polymorphs. (a) rutile, (b) anatase, (c) brookite.

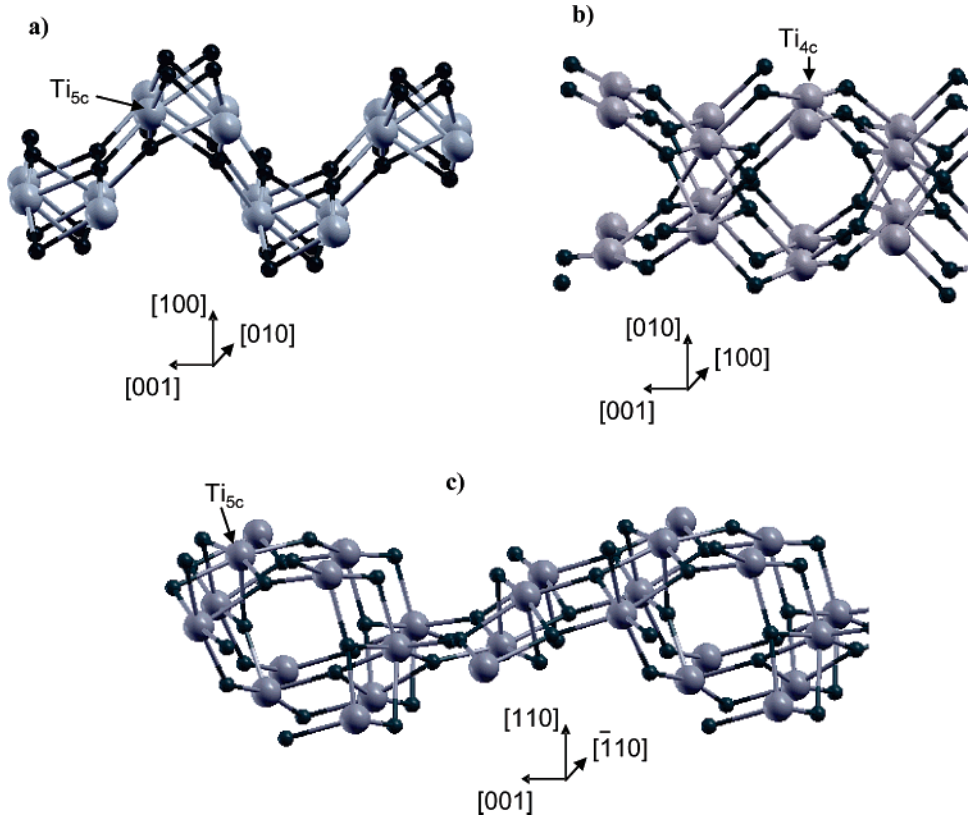

Figure 2. Structure of low-index surfaces for the brookite TiO_2 phase. (a) (100), (b) (010), (c) (110).

2. Structures

Brookite, the third natural form together with rutile and anatase polymorphs of TiO_2, has a complex structure. It has eight formula units in the orthorhombic cell (space group *Pbca*). Brookite formation may be envisioned as the joining of distorted TiO_6 octahedra sharing three edges. On the other hand, the TiO_6 octahedra in the rutile phase form chains that share edges along the *c* direction and share vertexes in the *ab* plane, while in the anatase structure the octahedra form zigzag chains along the *a* and *b* directions with each octahedron sharing four edges. The arrangement of these three polymorphs is depicted in Figure 1. Therefore, the essential difference with rutile and anatase is that, in brookite, there are six different Ti−O bond lengths.

The surface structures of brookite have been modeled by unreconstructed (truncated bulk) slab models using the calculated equilibrium geometry. As these surfaces have different number of atoms in each layer, after the corresponding convergence tests, the low-index surfaces were periodically modeled along *x*- and *y*-directions but with different thickness in the *z*-direction. The relaxation of these surfaces has been taken into account by optimizing all the layers of the slab.

This study explores the (100), (010), and (110) surfaces for the brookite phase. The (100) and (010) surfaces are represented by 12 atomic layers while the (110) surface is simulated by 24 layers. A schematic representation of these three low-index surfaces is depicted in Figure 2. The truncation of the octahedra

TABLE 1: Structural Data of Brookite Phase[a]

	exp[45]	calc
a (Å)	9.184	9.276
b (Å)	5.447	5.502
c (Å)	5.145	5.197
V (Å^3)	32.2	33.0
B_0 (GPa)	255[22]	220
B_0'	4[22]	3.7

[a] a, b, and c are the lattice parameters; V is the molecular volume; B_0 is the bulk modulus and B_0' is its first derivative with pressure.

renders different coordination combinations for the outermost titanium cations. Depending on the slice of the brookite surface, the (010) and (110) surfaces may be either oxygen- or titanium-terminated, the oxygen-terminated surfaces being the more stable. For this reason, only the oxygen-terminated surfaces are considered in this study. For the (010) surface the two top layers of oxygen ions are 2-fold coordinated (O_{2c}, O'_{2c}) and in the third layer, the titanium ions are 4-fold coordinated (Ti_{4c}). This termination is also the most stable of the studied surfaces. The ideal (110) brookite surface is characterized by the presence of pairs of coordinative unsaturated ions, i.e., 5-fold coordinated Ti (Ti_{5c}) and two types of 2-fold coordinated oxygen ions (O_{2c}, O'_{2c}), these atoms having only one cleaved bond. The (100) surface has a sawtooth profile and exhibits five coordinated Ti ions (Ti_{5c}) and 2-fold coordinated oxygen ions (O_{2c}); these atoms have one broken bond. In this case, only oxygen-terminated stoichiometric models can be built.

3. Computational Strategy

Calculations were performed with the CRYSTAL03 program package.[33] The standard 6-31G basis set was selected for the oxygen atom. For the titanium atom, the 6-31G basis set developed by Rassolov et al[34] was selected, as in a previous paper.[35] Becke's three-parameter hybrid nonlocal exchange functional[36] combined with the Lee−Yang−Parr gradient-corrected correlation functional, B3LYP,[37] has been used. The effects of the Fock exchange on the electronic structures of the TiO_2 have been recently explored, shifting the part of HF exchange in the DFT energy to obtain high-quality values of band gap, character of valence and conduction bands, and position of surface-induced states.[38] Nevertheless, the standard B3LYP hybrid method has been extensively used for molecules and also provides an accurate description of crystalline structures in regard to bond lengths, binding energies, and band gap values.[39]

To take into account the effect of pressure on this system, all the geometric parameters (a, b, c, and the nine internal positions) were optimized at a number of fixed volumes (V) in the range $0.88 < V/V_0 < 1.12$, where V_0 is the equilibrium unit-cell volume. The shrinking factor ($S = 12$) has been used to ensure an energy change less than the SCF convergence threshold 10^{-6} a.u. The computed (E, V_c) pairs were then used to calculate the pressure−volume data by minimizing the static Gibbs energy with respect to V at selected pressure values in the range 0−40 GPa. Values of the zero-pressure bulk modulus and its pressure derivative, B_0 and B_0', were also generated by means of a numerical fitting procedure consistent with the Birch−Murnaghan EOS.[40] This computational scheme allows the incorporation of temperature effects in the static calculation by means of the Debye theory implemented in the Gibbs program.[41]

The band structures have been obtained along the appropriate high-symmetry paths of the Brillouin zone for the orthorhombic primitive system.[42] The XCrysDen program[43] has been used to draw the band structure diagrams.

TABLE 2: Optimized Atomic Fractional Coordinates for the Brookite Phase Compared with Experimental Values from Literature. In Parenthesis, the Calculated Values for the Experimental Volume

		x		y		z	
atom		exp	this work	exp	this work	exp	this work
Ti	[a]	0.1296	0.1290 (0.1292)	0.0972	0.0898 (0.0907)	−0.1371	−0.1459 (−0.1459)
	[b]	0.127		0.113		−0.127	
	[c]	0.1289		0.0972		−0.1372	
O1	[a]	0.0101	0.0119 (0.0114)	0.1486	0.1500 (0.1511)	0.1824	0.1775 (0.1795)
	[b]	0.010		0.155		0.180	
	[c]	0.0095		0.1491		0.1835	
O2	[a]	0.2304	0.2290 (0.2300)	0.1130	0.1079 (0.1100)	−0.4629	−0.4704 (−0.4701)
	[b]	0.230		0.105		0.465	
	[c]	0.2314		0.1110		−0.4638	

[a] Reference 46. [b] Reference 47. [c] Reference 45.

4. Results and Discussion

4.1. EOS Fittings and Local Compressibility. A good description of the static equilibrium geometry is a requirement to validate the interpretation of volume-related bulk properties in terms of local magnitudes. Table 1 includes the structural parameters and bulk properties for the brookite. Comparison with updated experimental cell parameters reveals that our computations are sufficiently accurate, with deviations from the observed values never larger than 1%. The computed equilibrium zero-pressure value of the unit-cell volume is 33.0 Å^3 (2.5% larger than the experimental volume). Since a very high number of independent structural parameters of brookite were optimized, an isotropic variation of the unit-cell volume was carried out to obtain the minimum energy by varying only the diagonal elements of the matrix of fundamental vectors.[44] This optimization process was carried out until the convergence in energy achieved 10^{-4} a.u. Zero-pressure optimized fractional coordinates are in excellent agreement with the experimental values[45−47] and are presented in Table 2. The results show that the atomic internal coordinates also vary isotropically with pressure.

The theoretical determination of the stability and structure of materials under conditions that are difficult to reproduce in the laboratory is an added value of the present calculations. To our knowledge only one recent experimental value of bulk modulus larger than our theoretical value of 220 GPa has been reported for the brookite phase, namely that of 255 GPa by Luo et al,[22] which is also larger than that reported by Swamy et al (211 GPa).[21] Note that thermal effects have been considered, since temperature can play an important role in the modification of structural parameters and in the localization of thermodynamic phase boundaries, affecting, in different ways, the free energy of the several phases. In this sense, thermal effects at 300 K only decrease the B_0 of the phases by about 5% of their value. For comparison purposes, the bulk moduli and its first derivative for the rutile and anatase polymorphs were calculated. The computed bulk modulus for anatase of 200.2 GPa is in reasonable agreement with previous PW-LDA calculations, which found it to be about 190 GPa[48,49] and with the experimental value of 179 GPa.[50,51] The measured rutile bulk modulus was about 210 GPa,[52] with more recent studies verifying this value.[53] Therefore, the bulk modulus of anatase

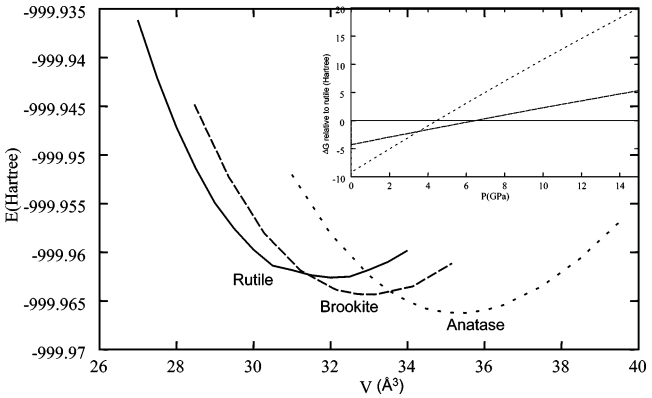

Figure 3. Internal energy (Hartree) versus the volume (in Å^3) per unit formula. The computed equation of state for the TiO_2 polymorphs is depicted in the inset.

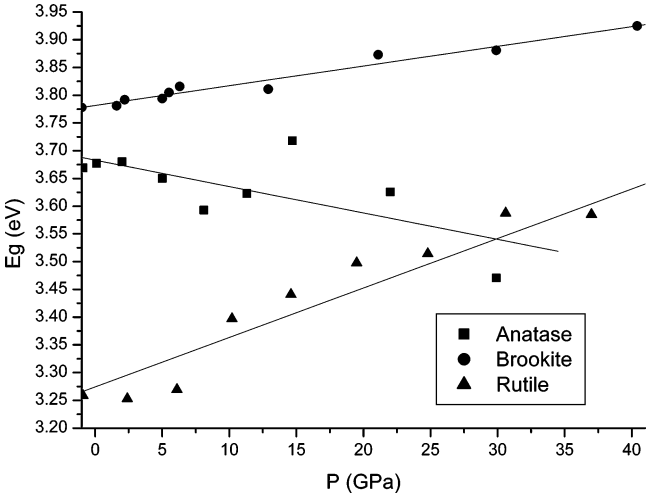

Figure 4. Effect of the pressure on the band gap energy for the TiO_2 polymorphs.

is lower than that of rutile (by about 6%), which is in agreement with the experiment.

The values of internal energy versus the volume for the TiO_2 polymorphs are plotted in Figure 3, together with the computed equation of state in the inset of the same figure. The present calculations predict that the anatase-to-brookite transformation occurs at about 3.8 GPa, while the rutile-to-brookite transition occurs around 6.2 GPa. In accordance with experimental observations[54] and other theoretical studies,[25] these results are correctly predicting that anatase will undergo a phase transformation at lower pressures than rutile (for example, to the columbite transition).

4.2. Electronic Structure of Bulk Brookite. The band structures of brookite were constructed along the appropriate high-symmetry directions of the corresponding irreducible Brillouin zones using the calculated lattice parameters listed in Table 1.

A direct band gap of 3.78 eV was obtained in the present study for the brookite structure which is slightly larger than that of rutile and anatase. Mo et al.[55] calculated the electronic structure of TiO_2 by means of first-principle self-consistent OLCAO method reporting a direct band gap of 2.2 eV for the brookite. A band gap energy of 3.4 eV was experimentally estimated for brookite nanoparticles dispersed in water.[19] Other experimental results[56,57] provide a value of 3.2 eV. The upper valence band, VB, lying in the range of 1.93−6.34 eV consists of O 2p orbitals hybridized with Ti 3d orbitals. The top of the VB of brookite (−5.02 eV at Γ) is closer to that of rutile (−4.70 eV at Γ) rather than of anatase (−5.51 eV at X). The bottom of the conduction band, CB, (−1.24 eV at Γ), composed of the Ti 3d orbitals, shows the same trend. These results differ from those reported by Matsushima et al,[58] in which the VB and CB widths of brookite are more similar to those of anatase than of rutile. However, there is agreement with the order of the band gap values provided by their FLAPW method at DFT-GGA level for the three polymorphs,[57] though with lower values.

For the rutile phase, the corresponding band structure indicates that the minimum energy gap between the VB and the CB is direct at Γ with a value of 3.24 eV. This value is slightly higher than the experimental results (3.0 eV)[59] but more accurate than other theoretical calculations. The electronic structure of anatase is characterized by an indirect band gap of 3.59 eV,[60] since the bottom of the CB is found at Γ and the top of the VB near X. This value is in reasonable agreement with the experimental value of 3.2 eV.[61]

The effect of pressure on the band structures of the three polymorphs is also examined in the present study. The zero-pressure values of the band gap energy (E_g) are ordered as rutile (3.24 eV) < anatase (3.59 eV) < brookite (3.78 eV). Pressure affects the band gap value, E_g, in a different way for the polymorphs. E_g increases in the rutile and the brookite structures as the CB moves to higher energy values, due to the Ti−O bond shortening by the pressure effect and also by the higher repulsion between the involved orbitals. The E_g enlargement is more noticeable in rutile than in brookite. In contrast, Figure 4 shows a decrease in band gap energy with pressure in anatase, the band gap remaining indirect when the X point is approached at the bottom of the CB.[60] The calculations predict the same value (crossing) for anatase and rutile around 30 GPa.

TABLE 3: Structural Parameters of the Brookite TiO_2 (100), (010), and (110) Surfaces[a]

(100) surface		
structural parameter	(O_{2c})	(Ti_{5c})
Δx [001]	−0.015	−0.249
Δy [010]	−0.014	−0.319
Δz [100]	−0.090	−0.040
$E_{surf}^{unrelax}$	2.65	
E_{surf}^{relax}	1.27	
E_g	3.69	

(010) surface			
structural parameter	(O_{2c})	(O'_{2c})	(Ti_{4c})
Δx [001]	0.406	−0.268	−0.082
Δy [100]	0.010	−0.037	−0.058
Δz [010]	0.125	0.098	−0.329
$E_{surf}^{unrelax}$	1.80		
E_{surf}^{relax}	0.97		
E_g	4.63		

(110) surface			
structural parameter	(O_{2c})	(O'_{2c})	(Ti_{5c})
Δx [001]	0.052	0.239	0.385
Δy [$\bar{1}$10]	−0.022	0.108	0.022
Δz [110]	−0.118	0.140	−0.163
$E_{surf}^{unrelax}$	2.04		
E_{surf}^{relax}	1.16		
E_g	2.78		

[a] Displacements from their perfect lattice positions in the indicated directions of the external O and Ti ions (Å). Unrelaxed ($E_{surf}^{unrelax}$) and relaxed (E_{surf}^{relax}) surface energies (Jm^{-2}) for the several low-index planes and the corresponding band gap energy (eV) are also provided.

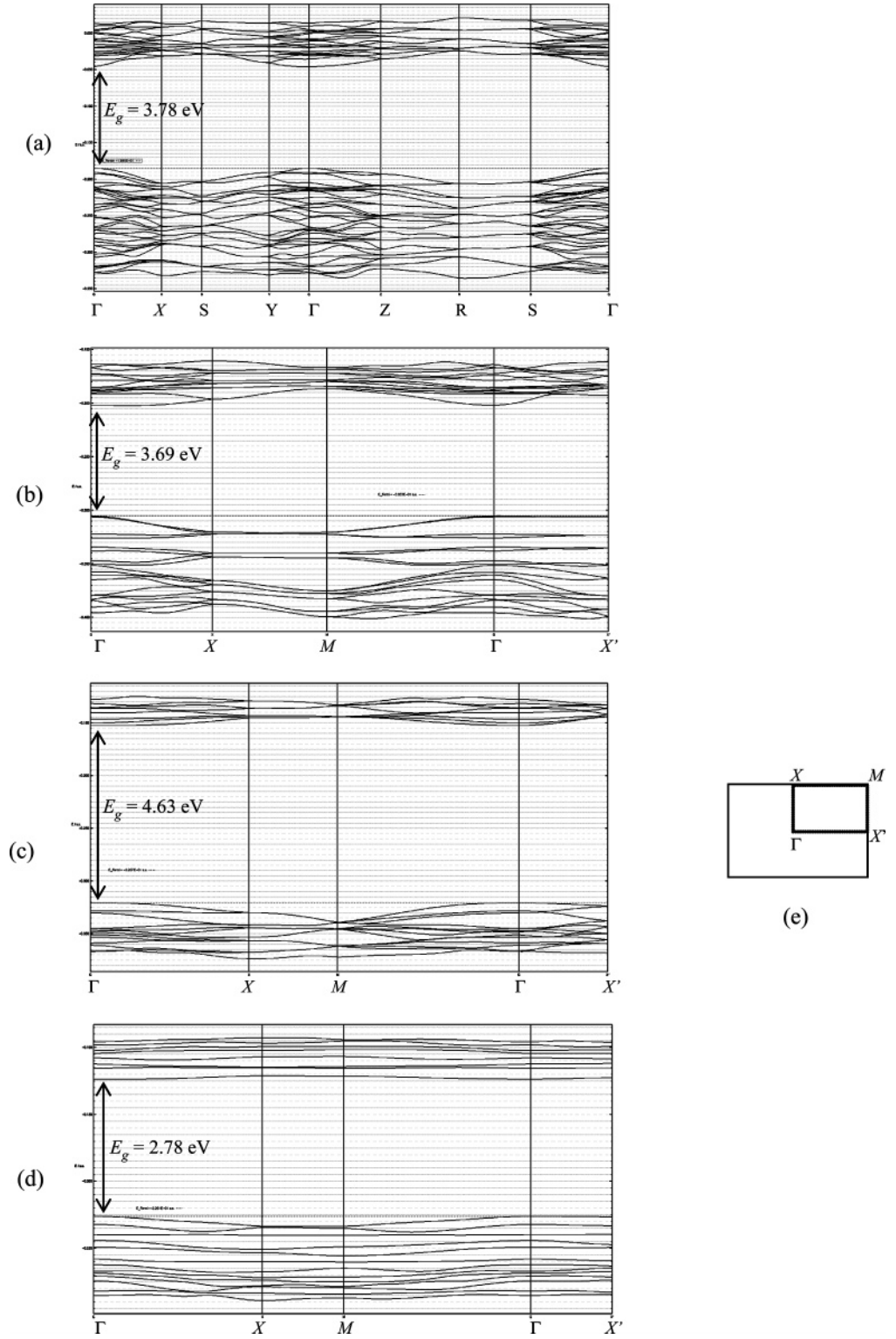

Figure 5. Band structure of the bulk brookite (a), and the slabs (b) (100), (c) (010), and (d) (110). The first Brillouin zone with high symmetry points for the surfaces is also shown (e).

4.3. Surface Properties. To confirm the convergence of the total energy with respect to slab thickness of the different surface models, the surface energy E_{surf} for several low-index planes of the brookite was calculated. As usual, E_{surf} is defined as the total energy per repeating cell of the slab minus the total energy of the same number of atoms of the perfect crystal, divided by the surface area per repeating cell of the two sides of the slab, i.e., $E_{surf} = (E_{slab} - nE_{bulk})/2A$.

Optimized geometric parameters for the brookite surfaces (100), (010), and (101) are summarized in Table 3. The largest changes are found along the [001] direction for the Ti_{5c} (110) 0.345 Å and (100) −0.249 Å; for the O_{2c} (010) 0.406 Å, and for the O'_{2c} (010) −0.268 Å and (110) 0.239 Å. Along the [010] direction, the major displacements were for Ti_{4c} (010) and Ti_{5c} (100), −0.329 Å and −0.319 Å, respectively. The gain in energy due to the optimization process is important between 43 and

52% of the surface energy. Table 3 also shows the unrelaxed ($E_{surf}^{unrelax}$) and the relaxed (E_{surf}^{relax}) surface energies for several low-index planes, and the corresponding E_g values. The lower part of the brookite CB has predominantly titanium character, due to 3d electrons, whereas the top of the VB is mainly due to the 2p oxygen states, as in the corresponding bulk. Assuming that the error due to the exchange and correlation functional is systematic to all the surfaces, some trends may be drawn from the results.

The analysis of the brookite slabs shows that the relaxation of atoms on the surface significantly decreases the surface energy values. As expected for the rutile and anatase slabs,[24,62,63] surface energies appear to be related to the presence of undercoordinated Ti atoms. The results shown in Table 3 indicate that surfaces with 4-fold coordinated Ti have higher energy than those with 5-fold coordinated Ti. Furthermore, the surface energy (of the relaxed structure) increases approximately with the rise in density of the undercoordinated Ti atoms. The stability of the brookite surfaces follows the following sequence: (010) < (110) < (100), for both unrelaxed and relaxed models.

Figure 5 shows the band structures of the studied surface slab models, i.e., the brookite (100), (010), and (110) surfaces, in addition to the first Brillouin zone with the high symmetry points. All the studied brookite surfaces present a direct gap, as in the bulk (the bottom of the CB and the top of the VB are located at Γ). The corresponding values are 3.69, 4.63, and 2.78 eV, respectively. The lower value of band gap energy for the (110) surface can be attributed to the minor stabilization of the Fermi energy showing the most flat VB topology. Rutile surfaces (110), (100), (101), and (001) have direct band gap at Γ. However, the anatase phase has the top of the VB near X in the (100), (101), and (110) surface terminations, and the VB is situated at M in (001). A comparison with the other two natural polymorphs shows that the average gap energy values, follows the sequence rutile < anatase < brookite, as in the corresponding bulks.

5. Conclusions

First-principles calculations based on the density functional theory under the B3LYP approximation of the natural brookite phase of TiO_2 were performed. The structural and electronic properties of the bulk, the response to hydrostatic pressure, and the low-index surfaces for the brookite phase were fully characterized. The findings provide valuable insights into the crucial link between the structure of a material on an atomic scale and its macroscopic properties. The main results may be summarized as follows:

(i) The response to hydrostatic pressure of the bulk structure of brookite in terms of the computed bulk modulus data is compared with other studied polymorphs and is consistent with the most reliable experimental results; the value increasing according to the sequence anatase, rutile, brookite. The present calculations predict the anatase-to-brookite transformation at about 3.8 GPa, while the rutile-to-brookite transition occurs around 6.2 GPa.

(ii) The nine optimized atomic internal coordinates of the brookite structure vary isotropically with pressure in the same way as the cell parameters. These facts are consistent with experimental data.

(iii) The analysis of the electronic structure for the bulk in terms of the calculated zero-pressure band gap energy shows a value of 3.78 eV.

(iv) Relaxed surface energies for several low-index planes of the brookite phase have been compared with those of anatase and rutile polymorphs. The brookite surface stabilities follow the sequence (010) < (110) < (100) for the unrelaxed as well as for the relaxed models.

(v) The analysis of the electronic structure for the studied surfaces of brookite shows a direct band gap in all of them. The minimum gap energy is found for the (110) surface.

It is hoped that this comprehensive study of the brookite TiO_2 polymorph will be helpful in further investigation of the properties of defects, impurities, thin films, surfaces, and interfaces in the TiO_2 system.

Acknowledgment. This study was supported by the DGI, (projects BQU2000-1425-C03-02 and BQU2003-04168-C03-03) and by the project GRUPOS04/28. L.G. gratefully acknowledges the Postdoctoral grant provided by the Universitat Jaume I. Use of the computer facilities of the Servei d'Informàtica (Universitat Jaume I) is also gratefully acknowledged.

References and Notes

(1) Nogami, G.; Shiratsuchi, R.; Ohkubo, S. *J. Electrochem. Soc*. **1991**, *138*, 751.
(2) Zhang, Z. L.; Kladi, A.; Verykios, X. E. *J. Phys. Chem.* **1994**, *98*, 6804.
(3) Topsoe, N. Y.; Dumesic, J. A.; Topsoe, H. *J. Catal.* **1995**, *151*, 241.
(4) Zhang, H. Z.; Banfield, J. F. *J. Mater. Chem.* **1998**, *8*, 2073.
(5) Topoglidis, E.; Cass, A. E. G.; Gilardi, G.; Sadeghi, S.; Beaumont, N.; Durrant, J. R. *Anal. Chem.* **1998**, *70*, 5111.
(6) Bach, U.; Lupo, D.; Comte, P.; Moser, J. E.; Weissortel, F.; Salbeck, J.; Spreitzer, H.; Gratzel, M. *Nature (London)* **1998**, *395*, 583.
(7) Bach, U.; Tachibana, Y.; Moser, J. E.; Haque, S. A.; Durrant, J. R.; Gratzel, M.; Klug, D. R. *J. Am. Chem. Soc.* **1999**, *121*, 7445.
(8) Yamazaki, S.; Hori, K. *Catal. Lett.* **1999**, *59*, 191.
(9) Yang, J.; Mei, S.; Ferreira, J. M. F. *J. Am. Ceram. Soc.* **2000**, *83*, 1361.
(10) Yang, J.; Mei, S.; Ferreira, J. M. F. *J. Mater. Res.* **2002**, *17*, 2197.
(11) Gratzel, M. *J. Photoch. Photobiol. C* **2003**, *4*, 145.
(12) Borgarello, E.; Kiwi, J.; Pelizzetti, E.; Visca, M.; Gratzel, M. *J. Am. Chem. Soc.* **1981**, *103*, 6324.
(13) Riegel, G.; Bolton, J. R. *J. Phys. Chem.* **1995**, *99*, 4215.
(14) Hurum, D. C.; Agrios, A. G.; Gray, K. A.; Rajh, T.; Thurnauer, M. C. *J. Phys. Chem. B* **2003**, *107*, 4545.
(15) Dachille, F.; Simons, P. Y.; Roy, R. *Am. Mineral.* **1968**, *53*, 1929.
(16) Zheng, Y. Q.; Shi, E. W.; Cui, S. X.; Li, W. J.; Hu, X. F. *J. Am. Ceram. Soc.* **2000**, *83*, 2634.
(17) Pottier, A.; Chaneac, C.; Tronc, E.; Mazerolles, L.; Jolivet, J. P. *J. Mater. Chem.* **2001**, *11*, 1116.
(18) Ohtani, B.; Handa, J.; Nishimoto, S.; Kagiya, T. *Chem. Phys. Lett.* **1985**, *120*, 292.
(19) Koelsch, M.; Cassaignon, S.; Guillemoles, J. F.; Jolivet, J. R. *Thin Solid Films* **2002**, *403*, 312.
(20) Bokhimi, X.; Morales, A.; Ortiz, E.; Lopez, T.; Gomez, R.; Navarrete, J. *J. Sol-Gel Sci. Technol.* **2004**, *29*, 31.
(21) Swamy, V.; Gale, J. D.; Dubrovinsky, L. S. *J. Phys. Chem. Solids* **2001**, *62*, 887.
(22) Luo, W.; Yang, S. F.; Wang, Z. C.; Wang, Y.; Ahuja, R.; Johansson, B.; Liu, J.; Zou, G. T. *Solid State Commun*. **2005**, *133*, 49.
(23) Linsebigler, A. L.; Lu, G. Q.; Yates, J. T. *Chem. Rev.* **1995**, *95*, 735.
(24) Diebold, U. *Surf. Sci. Rep*. **2003**, *48*, 53.
(25) Muscat, J.; Swamy, V.; Harrison, N. M. *Phys. Rev. B* **2002**, *65*, 224112.
(26) Francisco, E.; Bermejo, M.; Baonza, V. G.; Gerward, L.; Recio, J. M. *Phys. Rev. B* **2003**, *67*, 064110.
(27) Onishi, H.; Iwasawa, Y. *Surf. Sci.* **1994**, *313*, L783.
(28) Charlton, G.; Howes, P. B.; Nicklin, C. L.; Steadman, P.; Taylor, J. S. G.; Muryn, C. A.; Harte, S. P.; Mercer, J.; McGrath, R.; Norman, D.; Turner, T. S.; Thornton, G. *Phys. Rev. Lett.* **1997**, *78*, 495.
(29) Pang, C. L.; Haycock, S. A.; Raza, H.; Murray, P. W.; Thornton, G.; Gulseren, O.; James, R.; Bullett, D. W. *Phys. Rev. B* **1998**, *58*, 1586.
(30) Swamy, V.; Muscat, J.; Gale, J. D.; Harrison, N. M. *Surf. Sci.* **2002**, *504*, 115.
(31) Lindsay, R.; Wander, A.; Ernst, A.; Montanari, B.; Thornton, G.; Harrison, N. M. *Phys. Rev. Lett.* **2005**, *94*, 246102.

(32) Blanco-Rey, M.; Abad, J.; Rogero, C.; Mendez, J.; Lopez, M. F.; Martin-Gago, J. A.; de Andres, P. L. *Phys. Rev. Lett.* **2006**, *96*, 055502.
(33) Saunders: V. R.; Dovesi, R.; Roetti, C.; Orlando, R.; Zicovich-Wilson, C. M.; Harrison, N. M.; Doll, K.; Civalleri, B.; Bush, I. J.; D'Arco, P.; Llunell, M. *CRYSTAL2003 User's Manual*; University of Torino: Torino, 2003.
(34) Rassolov, V. A.; Pople, J. A.; Ratner, M. A.; Windus, T. L. *J. Chem. Phys.* **1998**, *109*, 1223.
(35) Beltrán, A.; Sambrano, J. R.; Calatayud, M.; Sensato, F. R.; Andrés, J. *Surf. Sci.* **2001**, *490*, 116.
(36) Becke, A. D. *J. Chem. Phys.* **1993**, *98*, 5648.
(37) Lee, C. T.; Yang, W. T.; Parr, R. G. *Phys. Rev. B* **1988**, *37*, 785.
(38) Zhang, Y. F.; Lin, W.; Li, Y.; Ding, K. N.; Li, J. Q. *J. Phys. Chem. B* **2005**, *109*, 19270.
(39) Hu, C.-H.; Chong, D. P. *Encyclopedia of Computational Chemistry*; Wiley: Chichester, 1998.
(40) Birch, F. *J. Geophys. Res.* **1952**, *57*, 227; **1978**, *83*, 1257.
(41) Blanco, M. A.; Francisco, E.; Recio, J. M. *The Gibbs Code*; miguel@carbono.quimica.uniovi.es, 1992.
(42) Bradley, C. J.; Crácknell, A. P. *The Mathematical Theory of Symmetry in Solids*; Clarendon Press: Oxford, 1972.
(43) Kokalj, A. *J. Mol. Graphics Modell.* **1999**, *17*, 176.
(44) Mackrodt, W. C. *J. Solid State Chem.* **1999**, *142*, 428.
(45) Meagher, E. P.; Lager, G. A. *Can. Mineral.* **1979**, *17*, 77.
(46) Wyckoff, R. W. G. *Crystal Structures*; Interscience Publishers: New York, 1960.
(47) Bokhimi, X.; Morales, A.; Aguilar, M.; Toledo-Antonio, J. A.; Pedraza, F. *Int. J. Hydrogen Energy*. **2001**, *26*, 1279.
(48) Dewhurst, J. K.; Lowther, J. E. *Phys. Rev. B* **1996**, *54*, R3673.
(49) Milman, V. *Properties of Complex Inorganic Solids*; Plenum Press: New York, 1997.
(50) Arlt, T.; Bermejo, M.; Blanco, M. A.; Gerward, L.; Jiang, J. Z.; Olsen, J. S.; Recio, J. M. *Phys. Rev. B* **2000**, *61*, 14414.
(51) Swamy, V.; Dubrovinsky, L. S. *J. Phys. Chem. Solids* **2001**, *62*, 673.
(52) Ming, L. C.; Manghnani, M. H. *J. Geophys. Res.* **1979**, *84*, 4777.
(53) Olsen, J. S.; Gerward, L.; Jiang, J. Z. *J. Phys. Chem. Solids* **1999**, *60*, 229.
(54) Haines, J.; Leger, J. M. *Physica B* **1993**, *192*, 233.
(55) Mo, S.-D.; Ching, W. Y. *Phys. Rev. B* **1995**, *55*, 13023.
(56) www.jpo.go.jp/shiryou/s_sonota/youjun_gijutsu/hikari_shokubai/06_gaiyou.pdf
(57) Wunderlicha, W.; Oekermannb, T.; Miaoc, L.; Hued, N. T.; Tanemurac, S.; Tanemurac, M. *J. Ceram. Proc. Res.* **2004**, *5*, 343.
(58) Matsushima, S.; Obata, K.; Yamane, H.; Yamada, K.; Nakamura, H.; Arai, M.; Kobayashi, K. *Electrochem.* **2004**, *72*, 694.
(59) Somartin, P. I.; Schwarz, K. *Inorg. Chem.* **1992**, *31*, 567.
(60) Calatayud, M.; Mori-Sanchez, P.; Beltrán, A.; Martín Pendás, A. *Phys. Rev. B* **2001**, *64*, 184118.
(61) Tang, H.; Berger, H.; Schmid, P. E.; Levy, F.; Burri, G. *Solid State Commun.* **1993**, *87*, 847.
(62) Ramamoorthy, M.; Vanderbilt D.; Kingsmith R. D. *Phys. Rev. B* **1994**, *49*, 16721.
(63) Barnard, A. S.; Zapol, P. *J. Phys. Chem. B* **2004**, *108*, 18435.